

Reinforcement learning modeling reveals a reward-history-dependent strategy underlying reversal learning in squirrel monkeys

Bilal A. Bari¹, Megan J. Moerke², Hank P. Jedema², Devin P. Effinger³,
Jeremiah Y. Cohen¹, Charles W. Bradberry²

¹*The Solomon H. Snyder Department of Neuroscience, Brain Science Institute, Kavli Neuroscience Discovery Institute, Johns Hopkins University, Baltimore, MD*

²*NIDA Intramural Research Program, 251 Bayview Blvd, Suite 200, Baltimore, MD 21224, USA*

³*Department of Pharmacology, University of North Carolina at Chapel Hill, Chapel Hill, NC
Correspondence: Charles W. Bradberry, charles.bradberry@nih.gov*

Funding Sources: This work was supported by R01DA042038 (J.Y.C. and B.A.B.), R01NS104834 (J.Y.C. and B.A.B.), T32GM007309 (B.A.B.), and the NIDA Intramural Research Program (M.J.M., H.P.J., D.P.E., and C.W.B.).

Conflict of Interest: None

Author Contributions: B.A.B. contributed to Conceptualization, Formal Analysis, Methodology, Software, Visualization, Writing - Original Draft, and Writing - Review & Editing. M.J.M. contributed to Data Curation, Investigation, Methodology, and Writing - Review & Editing. H.P.J. contributed to Data Curation, Investigation, Methodology, and Writing - Review & Editing. D.P.E. contributed to Data Curation, Investigation, and Methodology. J.Y.C. contributed to Conceptualization, Supervision, and Writing - Review & Editing. C.W.B. contributed to Conceptualization, Funding Acquisition, Project Administration, Resources, Supervision, and Writing - Review & Editing.

1 Abstract

2 Insight into psychiatric disease and development of therapeutics relies on behavioral tasks that study similar
3 cognitive constructs in multiple species. The reversal learning task is one popular paradigm that probes flexible
4 behavior, aberrations of which are thought to be important in a number of disease states. Despite widespread
5 use, there is a need for a high-throughput primate model that can bridge the genetic, anatomic, and behav-
6 ioral gap between rodents and humans. Here, we trained squirrel monkeys, a promising preclinical model, on an
7 image-guided deterministic reversal learning task. We found that squirrel monkeys exhibited two key hallmarks
8 of behavior found in other species: integration of reward history over many trials and a side-specific bias. We
9 adapted a reinforcement learning model and demonstrated that it could simulate monkey-like behavior, capture
10 training-related trajectories, and provide insight into the strategies animals employed. These results validate
11 squirrel monkeys as a model in which to study behavioral flexibility.

12 **Keywords:** reversal learning, reinforcement learning, squirrel monkeys, decision making, behavioral modeling

13 Introduction

14 Psychiatry is in need of fundamental insights both so we may understand the psychological and neural basis of
15 disease and so we can develop novel therapeutics. Comparative neuroscience is one approach that has histori-
16 cally led to the discovery of safe and effective pharmaceuticals (Markou et al., 2009). One common procedure
17 is to combine animal models of psychiatric disease with commonly-used behavioral tasks, such as the forced
18 swim test or elevated plus maze. Compounds can then be tested for their ability to ameliorate modeled symp-
19 toms (Kaiser and Feng, 2015; Flint and Shifman, 2008; Crawley, 2008; Dawson and Tricklebank, 1995; Nestler
20 et al., 2002). While this approach has been fruitful, it has failed to fundamentally change our understanding
21 about disease or lead to the discovery of truly novel therapeutics (Pangalos et al., 2007; Fenton et al., 2003).
22 This is partly because preclinical behavioral models represent a major bottleneck in drug development (Tallman,
23 1999). Since psychiatric diseases affect higher-order cognitive processes, designing tasks that translate drug ef-
24 fects from animal models to humans is nontrivial. The standard library of tasks were designed to probe intuitive
25 ideas about observable symptoms, not quantitative theories of cognitive processes.

26 A promising approach is to design behavioral tasks that probe the same psychological phenomena across species
27 (Pike et al., 2021). These tasks may use different stimuli and motor responses, but attempt to isolate the same
28 neurocomputational mechanisms. Theories about the relevant cognitive processes are used to form and test ex-
29 plicit hypotheses, in the form of models, about behavioral strategies (Wilson and Collins, 2019; Daw et al., 2011;
30 Heathcote et al., 2015). From the perspective of computational psychiatry, these models in turn allow us to un-
31 derstand and quantify aberrant information processing in disease (Huys et al., 2016; Aylward et al., 2019; Ger-
32 shman and Lai, 2020; Mason et al., 2017; Redish, 2004; Radulescu and Niv, 2019), as well as effects of therapy
33 (Michely et al., 2020; Frank et al., 2007; Paulus et al., 2016).

34 Reversal learning is one popular task that is amenable to theory-based computational modeling (Behrens et al.,
35 2007; Soltani and Izquierdo, 2019). In common variants of this task, subjects are presented with a choice be-
36 tween two stimuli, one associated with a high-value outcome (e.g. high probability or large volume of reward)
37 and the other associated with a low-value outcome. Subjects begin the task with no knowledge about which
38 stimulus is the better option. On each trial, subjects select one stimulus, receive the associated outcome, and
39 repeat this process. Through trial-and-error, subjects learn the values of each stimulus. After some time, the
40 two stimuli reverse in association (hence, reversal learning), so that the previously low-value stimulus becomes
41 the high-value stimulus and vice versa. Importantly, these reversals are not cued, necessitating continual trial-
42 by-trial learning to maximize reward. This task design is thought to engage mechanisms of flexible and rapid
43 learning, impairments of which are implicated in a wide range of psychiatric disease (Swanson et al., 2000; Huys
44 et al., 2013; Aylward et al., 2019; Remijnse et al., 2006; Brigman et al., 2009; Leeson et al., 2009; Izquierdo and
45 Jentsch, 2012), including addiction (Porter et al., 2011; Ersche et al., 2011).

46 Although behavior on these tasks is typically reported using simple summary statistics (average performance,
47 trials to reach a criterion, etc.), richer insight can be gleaned with reinforcement learning modeling. Reinforce-
48 ment learning is a framework that formalizes learning from environmental feedback (Sutton and Barto, 1998),
49 and has provided a number of tractable algorithms that have delineated numerous structure-function relation-
50 ships in the nervous system (Schultz et al., 1997; Samejima et al., 2005; Bari et al., 2019; Ottenheimer et al.,
51 2020; Grossman et al., 2020; O'Doherty et al., 2004). Among the most commonly-applied algorithms are the
52 class that iteratively learn stimulus values over many trials and choose based on the relative values of the stim-
53 uli. Reinforcement learning models of reversal learning have been used to explain behavioral data in species as
54 diverse as rodents (Harris et al., 2020; Metha et al., 2020), macaques (Costa et al., 2016), and humans (Kanen
55 et al., 2019). Importantly, reinforcement learning models are generative models — that is, they are capable of
56 simulating behavior, a premise which we capitalize on in this manuscript.

57 Here, we trained squirrel monkeys on a deterministic image-based reversal learning task. Squirrel monkeys are
58 New World primates widely used in biomedical research, primarily due to their small size (<1kg), ease of han-

59 dling, and adaptation to laboratory conditions (Abee, 2000). From the perspective of comparative neuroscience,
60 squirrel monkeys help span the massive genetic, anatomical, and behavioral gap between rodents and humans
61 (Boinski, 1999). They may also prove to be a useful preclinical model for development of optogenetic-based in-
62 terventions (O'Shea et al., 2018).

63 Our objective was to determine if squirrel monkeys solve reversal learning tasks using a strategy compatible
64 with trial-by-trial reinforcement learning, and to isolate parameters of cognitive flexibility to employ in future
65 studies. First, we demonstrate that squirrel monkeys do not adopt the optimal win-stay/lose-shift strategy re-
66 quired to optimize reward accumulation in this task but rather integrate reward over many trials. We fit a num-
67 ber of reinforcement learning models and found that a standard Rescorla-Wagner model fit best, similar to re-
68 versal learning models in other species. We show that this model simulates realistic behavior, providing a con-
69 vincing platform for making inferences about behavioral strategy. Finally, we use the recovered parameters to
70 define how the behavioral strategy develops with training.

71 Methods

72 Subjects

73 A total of 13 (9 of which met behavioral criteria) adult male squirrel monkeys (*Saimiri sciureus*) with less than
74 1 year of training on behavioral touchscreen tasks were housed individually under controlled temperature and
75 humidity on a 12/12-h light-dark cycle (lights on from 0700 to 1900h). Monkeys weighed 867-1113 g (mean:
76 965 g) and were maintained on a diet of primate chow (LabDiet High Protein Monkey Biscuits; PMI Feeds, St.
77 Louis, MO) with continuous access to water in the home chamber. Environmental enrichment, including fresh
78 fruits and vegetables, was provided on a daily basis. The maintenance and experimental use of animals was car-
79 ried out in accordance with the 2011 Guide for Care and Use of Laboratory Animals. All experimental protocols
80 were approved by the Animal Care and Use Committee of the National Institute on Drug Abuse Intramural Re-
81 search Program.

82 Apparatus

83 Experiments were conducted in sound-attenuating chambers equipped with a 15" touchscreen (Elo TouchSys-
84 tems, Menlo Park, CA), mounted in a panel 14.25" from the floor of the chamber. Centered 1.5" below the
85 touchscreen and extending 2" into the chamber was a well into which measured volumes of 30% sweetened con-
86 densed milk (Eagle Foods, Richfield, OH) could be delivered through a line connected to a syringe pump (Har-
87 vard Apparatus, South Natick, MA) located outside the chamber. Monkeys were seated in custom-built acrylic
88 chairs facing the touchscreen panel. A computer and software program (E-Prime Professional 3.0; Psychology
89 Software Tools, Inc., Sharpsburg, PA) controlled the parameters of the experimental program and data collec-
90 tion.

91 Behavioral task and training

92 Prior to introducing the reversal task, monkeys were trained on a task in which they chose between different
93 quantities of milk (0.075-0.3 ml/kg) represented by unique stimuli on the touchscreen. Monkeys registered a
94 choice by physically touching the display for 100 ms; this was paired with a tone and allocation of the associ-
95 ated reward into the well below the touchscreen. A house light and speakers inside the experimental chambers
96 provided illumination and white noise. Training sessions were generally carried out five days a week (Monday-
97 Friday) and lasted 30-60 min.

98 Following this training task, monkeys conducted an image-based deterministic reversal learning task. These
99 sessions began with a Discrimination block, in which monkeys were presented with two novel images selected
100 randomly from a large library of images. One image was associated with a big reward (large volume of milk;
101 the ‘correct’ choice) and the other image was associated with a small reward (small volume of milk; the ‘incor-
102 rect’ choice). Monkeys registered a choice by physically touching one of the visual stimuli on the display and
103 received the associated reward from a reward port. Following an 8-12 second intertrial interval, the images were
104 presented again on the next trial, with left/right positions randomized between trials. Monkeys made choices
105 until they reached a performance threshold of 80% correct in the past 15 trials, after a minimum 20 trial block
106 length. Once this threshold was reached, a Reversal block was initiated, in which the two image associations re-
107 versed so the image previously associated with big reward was now associated with small reward, and vice versa
108 for the other image. Monkeys again performed until they reached the performance threshold, at which point a
109 new Discrimination block was initiated and two new images were randomly sampled from the library. Monkeys
110 typically performed for 150 trials, although some sessions were shorter due to reduced motivation. The large re-
ward (0.13-0.24 ml/kg) was four times larger than the small reward (0.03-0.06 ml/kg).

112 Data analysis

113 All 13 monkeys completed at least 60 sessions and at least 1 block per session on average. Monkeys that reached
114 an average performance threshold of 54% across all reward blocks and all sessions were included, yielding 9 mon-
115 keys in the final dataset. Monkeys performed an average of 121 sessions (range 66-135).

116 All choices that yielded big (small) reward were labeled as correct (incorrect). Performance was defined as the
117 fraction of correct choices in a session. To generate reward history regressions, we arbitrarily coded one image
118 as “image 0” and the other image as “image 1” for each set of presented images and fit the following random
119 effects logistic regression

$$\log \left(\frac{P(c_1(t))}{1 - P(c_1(t))} \right) = \sum_{i=1}^{15} \beta_i (R_1(t-i) - R_0(t-i)) + \beta_{int}$$

120 where $c_1(t) = 1$ for a choice to “image 1” and 0 for a choice to “image 0”. $R(t) = 1$ if big reward was delivered
121 for that image on trial t and 0 otherwise. We included monkey-level and session-level (nested within monkey)
122 random effects for the intercept.

123 We generated errorbars for performance within blocks (Figures 2D, 4D) by computing bootstrapped 95% confi-
124 dence intervals from 1,000 bootstrap samples of the mean.

125 In generating image-based win-stay/lose-shift and mutual information metrics, we excluded the first trial of each
126 Discrimination block, as new images were presented on these trials. The mutual information between stay/shift
127 (to image) and reward on the previous trial was calculated as

$$\begin{aligned}
 I(R, S) &= H(S) - H(S|R) \\
 H(S) &= - \sum_{s \in S} P(s) \log_2(P(s)) \\
 &= -(P(\text{switch}) \log_2(P(\text{switch})) + P(\text{stay}) \log_2(P(\text{stay}))) \\
 H(S|R) &= \sum_{r \in R} H(S|r) P(r) \\
 &= -(P(\text{switch|win}) \log_2(P(\text{switch|win})) + P(\text{stay|win}) \log_2(P(\text{stay|win}))) P(\text{win}) + \\
 &\quad -(P(\text{switch|lose}) \log_2(P(\text{switch|lose})) + P(\text{stay|lose}) \log_2(P(\text{stay|lose}))) P(\text{lose})
 \end{aligned}$$

128 where $I(R, S)$ is the mutual information, $S = \{\text{switch, stay}\}$ on the current trial, and $R = \{\text{win, lose}\}$ on the
129 previous trial.

130 Side bias was defined as $2 \cdot |\frac{N_r}{N_r+N_l} - 0.5|$ where N_r and N_l are the total rightward and leftward choices in a
131 session, respectively. Side bias = 0 if there are an equal number of leftward/rightward choices and 1 if all choices
132 are exclusively to one side. The entropy of the side chosen distribution was calculated as

$$\begin{aligned}
 H(C) &= - \sum_{c \in C} P(c) \log_2(P(c)) \\
 &= -(P(\text{leftward}) \log_2(P(\text{leftward})) + P(\text{rightward}) \log_2(P(\text{rightward})))
 \end{aligned}$$

133 where $C = \{\text{leftward, rightward}\}$.

134 All regressions relating behavioral metrics to sessions number were random effects linear regressions with monkey-
135 level random effects for slope and intercept.

136 Reinforcement learning models

137 We developed a number of reinforcement learning models based on the Rescorla-Wagner model. Our chosen
138 model took the following form for updating image values

$$\begin{aligned}
 \delta(t) &= R(t) - V_{\text{chosen}}(t) \\
 V_{\text{chosen}}(t+1) &= V_{\text{chosen}}(t) + \alpha \cdot \delta(t) \\
 V_{\text{unchosen}}(t+1) &= V_{\text{unchosen}}(t)
 \end{aligned}$$

139 where values were initialized with $V_i = 0$ at the beginning of each Discrimination block. In this model, the cho-
140 sen image's value is updated based on the discrepancy between prediction and reward (reward prediction error,
141 $\delta(t)$). The unchosen image's value remains unchanged. Image values were fed into a softmax function to gener-
142 ate choices according to

$$\begin{aligned}
 P(c(t) = \text{rightward}) &= \frac{1}{1 + e^{-\beta(V_{\text{rightward}} - V_{\text{leftward}}) - \text{bias}}} \\
 P(c(t) = \text{leftward}) &= 1 - P(c(t) = \text{rightward})
 \end{aligned}$$

143 We fit a number of model variants. First, we considered a set of noise models testing whether behavior could
144 be explained as random, biased, perseverative (1-trial-back choice autocorrelation), or biased + perseverative.
145 Within the space of Rescorla-Wagner models, we considered models with all possible combinations of the follow-
146 ing: one learning rate, two learning rates (separate learning of positive and negative reward prediction errors),
147 forgetting of unchosen image values to 0, rewards coded as [0.25 1] (since the small reward was 25% the volume
148 of the large reward; only for models with forgetting), and learning of action values (i.e. learning values for left-
149 ward/rightward actions). Each of these models also included permutations for nuisance parameters (none, side
150 bias, perseveration, or side bias + perseveration). We additionally considered a set of models that augmented
151 each model to allow for a mixture of image-based win-stay/lose-shift and reinforcement learning. We consid-
152 ered one final model (a variant of our chosen model) that explicitly accounted for a reversal mechanism. In this
153 model, reward prediction errors symmetrically updated image values - if one image value was increased by $\delta(t)$,
154 the other image value was decreased by $\delta(t)$, while bounding image values by [0 1]. In all models reward val-
155 ues were coded as 0 and 1 for small reward and big reward, respectively (except for the variant where they were
156 coded as [0.25 1]). In total, we considered 105 model variants.

157 We developed a metric, the maximal trial-by-trial change in $P(\text{choice})$, to capture the interaction between the
158 learning rate, α , and the inverse temperature, β (Figure 6F,J, S6C). For a given α and β , we assumed the largest
159 reward prediction error, $\delta(t) = 1$. This yields $V_{\text{chosen}}(t+1) = V_{\text{chosen}}(t) + \alpha \cdot \delta(t)$, which can be simplified as
160 $V_{\text{chosen}}(t+1) - V_{\text{chosen}}(t) = \alpha$. In other words, the value function is increased by α in response to the largest pos-
161 sible reward prediction error in this task. We then calculated the change in $P(\text{choice})$ around the inflection point
162 of the softmax function (at $P(\text{choice}) = 0.5$) since the slope is steepest at this point. This yields the maximum
163 trial-by-trial change in $P(\text{choice})$.

$$\Delta P(\text{choice}) = \frac{1}{1 + e^{-\beta \cdot \alpha/2}} - \frac{1}{1 + e^{-\beta \cdot -\alpha/2}}$$

164 Model fitting

165 Models were fit to individual session data with maximum likelihood estimation, with 10 starting points to avoid
166 finding local minima. To determine which models fit the data most parsimoniously, we used the Bayesian infor-
167 mation criterion, which penalizes models with additional parameters. The above reinforcement learning model
168 fit best for the most monkeys (Table S1).

169 This model is notable for several reasons. First, none of the noise models fit best for the monkeys included in
170 this dataset. Because Bayesian information criterion, relative to other metrics (like Akaike information crite-
171 rion), favors simpler models, this suggests that Rescorla-Wagner-like learning is a key feature of behavior. Sec-
172 ond, although reinforcement learning models with two learning rates are often fit to animal and human data,
173 we found that none of the models with two learning rates were selected. Third, none of the win-stay/lose-shift
174 models provided better fits than the complementary model variants without win-stay/lose-shift. This includes
175 four win-stay/lose-shift models that did not include Rescorla-Wagner-style learning (a mixture of the four noise
176 models + win-stay/lose-shift).

177 Model recovery

178 For the best model, we took the parameter estimates for each session and generated fictive data according to the
179 same model. We then fit all 105 models to this synthetic dataset and found that the true generative model was
180 selected for 9 of the 9 simulated monkeys. This shows that our model recovery procedure could indeed recover
181 our chosen model.

182 We also conducted a parameter recovery exercise with these models and found that the difference between ac-
183 tual and recovered parameters had a mode of 0 for all three parameters.

184 Hierarchical Bayesian model fitting

185 To obtain partially-pooled parameter estimates (i.e., less noisy estimates, especially since α and β tend to com-
186 pensate for one another (Daw et al., 2011; Ballard and McClure, 2019)), we refit the best reinforcement learn-
187 ing model using a hierarchical Bayesian framework. We used MATLAB (Mathworks), the probabilistic pro-
188 gramming language Stan (<https://mc-stan.org>), and the MATLAB interface, MatlabStan (<https://mc-stan.org/users/interfaces/matlab-stan>). We constructed hierarchical models separately for each monkey, with
189 monkey-level parameters to govern session-level parameters for learning. Priors over monkey-level parameters,
190 from which session-level means were drawn, were set as

$$\begin{aligned}\alpha &\sim \text{Beta}(1.2, 1.2) \\ \beta &\sim \text{Gamma}(4.82, 0.88) \\ \text{bias} &\sim \text{Normal}(0, 1)\end{aligned}$$

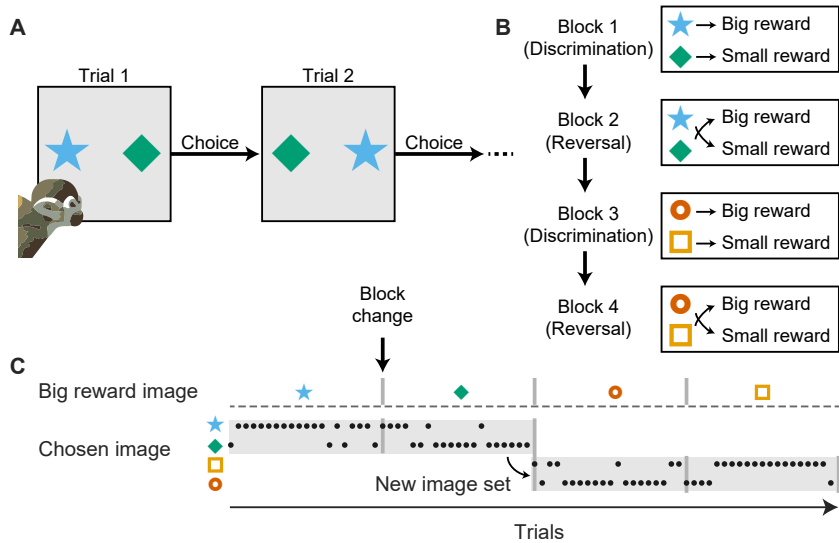
192 where the priors for α and β were taken from the literature (Kanen et al., 2019; Den Ouden et al., 2013; Gersh-
193 man, 2016). The gamma distribution was parameterized in terms of shape and scale. For all monkey-level vari-
194 ances, we used Cauchy⁺(0, 1). For session-level α and β , we again used beta and gamma distributions, reparam-
195 eterized in terms of mean and variance with parameters drawn from monkey-level distributions. Session-level
196 bias was normally distributed, with mean and variance drawn from monkey-level distributions. Parameter val-
197 ues reported in Figure 6 are the means of the session-level posteriors. Distributions in Figure 6A-C are posteri-
198 ors over monkey-level means.

199 Results

200 Reward history and side bias inform strategy

201 We developed a deterministic reversal learning task in which chaired squirrel monkeys chose between two simul-
202 taneously presented images for delivery of milk reward. Images were presented in blocks of trials, and in each
203 block, one image was associated with big reward and the other was associated with small reward. On each trial,
204 monkeys were presented with two images, each on the left/right half of a touchscreen and physically touching
205 an image yielded reward (Figure 1A). Selecting the big reward image (which we call the correct choice) for 80%
206 of the past 15 trials triggered a block transition, uncued to the monkey. Blocks switched between Discrimina-
207 tion blocks and Reversal blocks (Figure 1B). At the beginning of each Discrimination block, two images were
208 randomly selected from a large library of images and assigned to big/small reward. At the beginning of each Re-
209 versal block, the two images swapped reward contingencies. On average, sessions lasted for 146 (SD 14) trials
210 and monkeys completed 4.8 (SD 1.9) blocks.

211 The optimal strategy in this task is an image-based win-stay/lose-shift policy: select the same image if it yielded
212 big reward on the previous trial, switch if it yielded small reward. After training, monkeys reliably switched
213 their choices at block transitions, when contingencies switched (Figure 1C, S1A). However, although animals
214 performed significantly better than chance (Wilcoxon signed-rank test, $p < 0.01$), they performed worse than
215 win-stay/lose-shift, a optimal strategy that would yield the large reward on ~96% of trials (Figure 2A). To un-
216 derstand how monkeys solved this task, we fit logistic regression models to predict choice as a function of reward



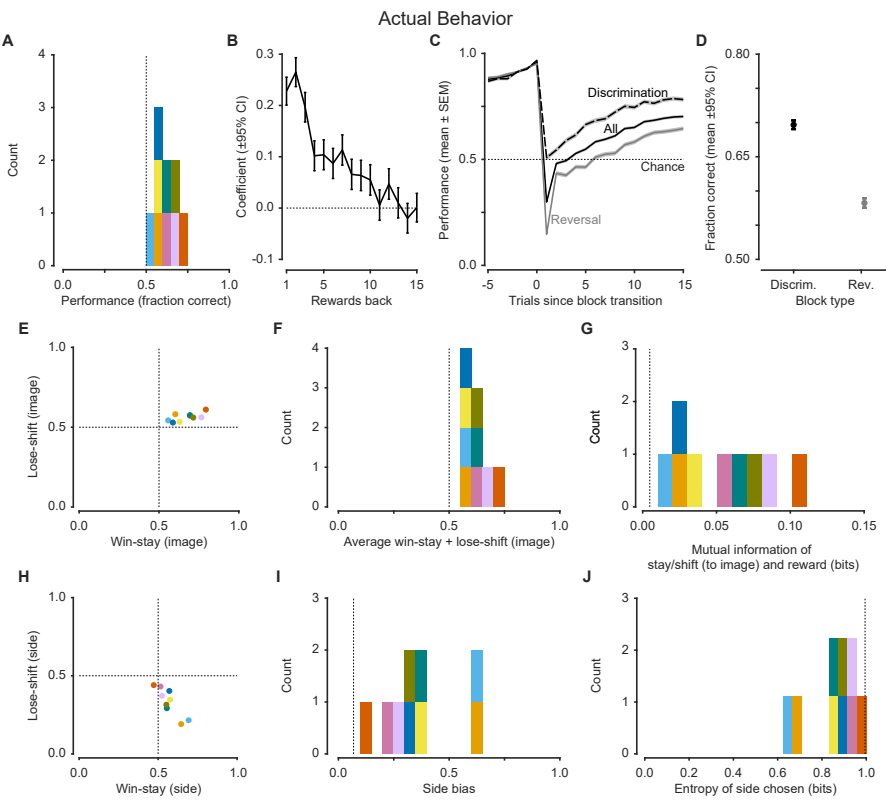


Figure 2: Behavioral features demonstrate reward sensitivity and side bias (A) Performance was significantly better than chance (50%, dashed line). (B) Logistic regression coefficients for choice as a function of reward history. (C) Performance at block transitions for all blocks, and separately for Discrimination and Reversal blocks. Relative to Reversal blocks, monkeys were faster to improve performance during new Discrimination blocks. The increase in performance prior to block transitions is because transitions were triggered by good performance. (D) Performance was better in Discrimination blocks relative to Reversal blocks. (E) Image-based win-stay and lose-shift were both greater than 0.5, demonstrating that animals learned from both wins (big reward) and losses (small reward) to guide decisions. (F) The average win-stay + lose-shift, which can be taken as a proxy for the strength of reward-guided behavior, was greater than 0.5 (dashed line). Values close to 0.5 are consistent with reward-insensitive behavior and values of 1.0 are consistent with a perfect win-stay/lose-shift strategy. (G) The mutual information between stay/switch and reward on the previous trial. Mutual information quantifies how much better we can predict the strategy (stay vs switch) if we know the reward received on the previous trial (dashed line is from simulated random behavior). (H) Side-based win-stay and lose-shift highlight a side bias, where animals largely stay. (I) Side bias, which is 1 if choices are exclusively to one side and 0 if they are uniformly split, was widely distributed (dashed line is from simulated non-side-biased behavior). (J) The entropy of the side chosen distribution showed a similarly wide distribution. Entropy of 1 indicates choices were uniformly split and entropy of 0 indicates choices were exclusively to one option (dashed line is from simulated non-side-biased behavior). Colors denote individual monkeys and are consistent between figures.

for reward-sensitive behavior. Consistent with prior analyses, animals demonstrated reward-sensitive behavior (Wilcoxon signed-rank test, $p < 0.01$). However, one shortcoming of this metric is it places equal emphasis on win-stay and lose-shift. Because $P(\text{lose})$ is fairly low in this task, behavior in response to losses does not impact overall performance as strongly as response to reward. To work around this pitfall, we computed the mutual information between reward on the previous trial and stay/switch behavior on the current trial, as it accounts for the base rate of $P(\text{lose})$ (Figure 2G). Perfect win-stay/lose-shift behavior results in 1 bit of information and reward-insensitive behavior results in 0 bits. Consistent with the average win-stay + lose-shift analysis, monkeys demonstrated reward-sensitive behavior (Wilcoxon signed-rank test, $p < 0.01$).

246 One notable behavioral suboptimality we observed was a bias towards a particular side (a rightward side bias
 247 can be seen in Figure S1A) (Friedman et al., 2017; Bari et al., 2019). To better understand this side bias, we
 248 quantified win-stay/lose-shift in side-based coordinates (Figure 2H). Most monkeys fell in the bottom-right quad-
 249 rant, consistent with a reward-insensitive tendency to favor a particular side (win-stay > 0.5 and lose-switch
 250 < 0.5, Wilcoxon signed-rank test, $p < 0.01$ for each). We quantified side bias with a side bias metric (0 for
 251 uniformly split choices, 1 for exclusive choice of one side) and observed a wide distribution, indicating an aver-
 252 age tendency for side biased behavior (Figure 2I; Wilcoxon signed-rank test, $p < 0.01$). The entropy of the side
 253 chosen distribution was similarly wide (1 bit for uniformly split choices, 0 bits for exclusive choice of one side;
 254 Figure 2J; Wilcoxon signed-rank test, $p < 0.01$).

255 Taken together, these results argue that monkeys solve this task by integrating reward over many trials to in-
 256 form choices, and that this strategy is corrupted by a side bias.

257 Monkeys develop reward sensitivity and reduce side bias with training

258 The wide range of performance allowed us to relate behavioral performance to the behavioral metrics we de-
 259 fined. First, we found that the average win-stay + lose-shift increased with better performance (linear slope
 260 0.82, $t_7 = 28.23$, $p < 0.0001$), consistent with the optimality of image-based win-stay/lose-shift (Figure 3A).
 261 Similarly, the mutual information between reward and stay/shift increased with performance (Figure 3B; lin-
 262 ear slope 0.50, $t_7 = 19.54$, $p < 0.0001$). Next, we focused on the side bias (Figure 3C). We found that for poor
 263 performance, side bias was generally high and decreased with improved performance (Mean: linear slope -1.98 ,
 264 $t_7 = -3.17$, $p = 0.016$). The entropy of the side chosen distribution increased with improved performance (Fig-
 265 ure 3D; Mean: linear slope 1.31, $t_7 = 2.84$, $p = 0.025$).

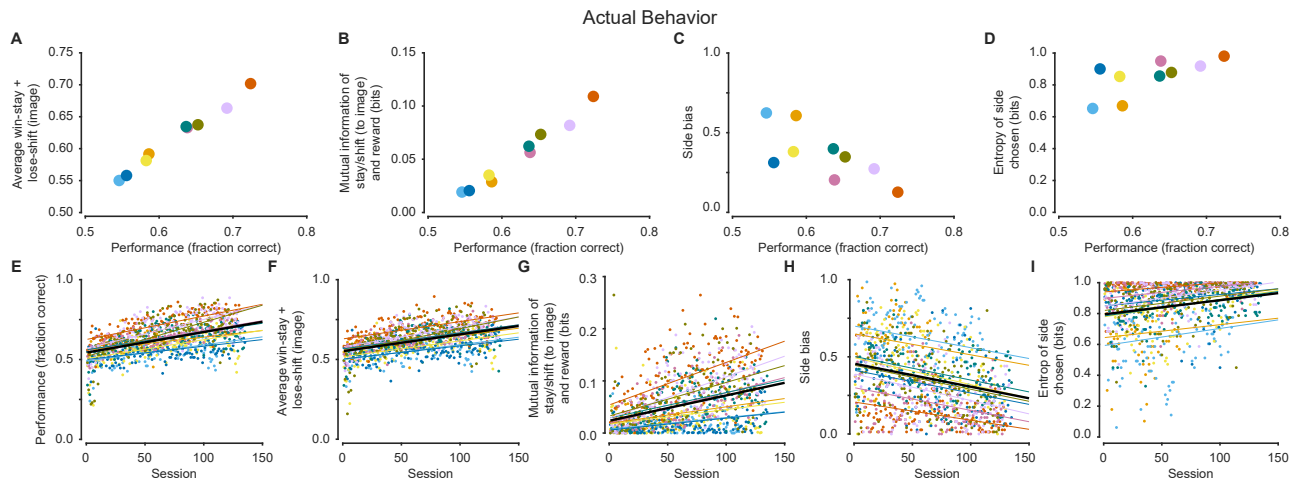


Figure 3: Relationship between performance, reward sensitivity, side bias, and training (A) The average win-stay + lose-shift increased with increased performance. (B) The mutual information between stay/shift and reward increased with performance > 0.5 . (C) Side bias was higher when performance was closer to 0.5 and reduced when performance was better. (D) Similarly, the entropy of the side chosen distribution increased (i.e. left/right choices become more random) when performance improved. (E) Performance improved with more sessions performed. (F) The average win-stay + lose-shift improved with training. (G) The mutual information between stay/switch and reward increased with training. (H) Side bias decreased with training. (I) Similarly, the entropy of the side chosen distribution increased with training. Black line shows the fixed effect and thin colored lines show individual monkey random effects. Colors denote individual monkeys and are consistent between figures.

266 The large number of sessions per monkey additionally allowed us to quantify the effects of training. First, we
 267 found that performance increased with the number of sessions (Figure 3E; linear slope 1.3×10^{-3} , $t_{1091} = 7.85$,

268 p < 0.0001). This was partly due to increased reward-sensitivity to images. The average win-stay + lose-shift
269 increased with training (Figure 3F; linear slope 1.1×10^{-3} , $t_{1091} = 11.04$, p < 0.0001). Similarly, the mutual
270 information between reward and stay/switch increased (Figure 3G; linear slope 4.86×10^{-4} , $t_{1091} = 5.58$, p
271 < 0.0001). The improvement in performance was also partly due to a decrease in side bias. The side bias de-
272 creased with training (Figure 3H; linear slope -1.5×10^{-3} , $t_{1091} = -8.51$, p < 0.0001). Similarly, the entropy of
273 the side chosen distribution increased with training (Figure 3I; linear slope 9.17×-4 , $t_{1091} = 6.64$, p < 0.0001).
274 In summary, monkeys improve with training, partly due to increased reward sensitivity to images, and partly
275 due to a decrease in side bias.

276 Reinforcement learning modeling captures key features of behavior

277 Since we found that monkeys integrated rewards over many trials, we adapted the Rescorla-Wagner model, a
278 commonly-used model in reinforcement learning (Rescorla, 1972). This model maintains a running estimate of
279 the values of images and chooses based on the relative values of the presented images. Image values are learned
280 by recency-weighted reward history, which allows the model to adapt behavior flexibly when reward contingencies change. We considered a number of model variants: equivalent vs differential learning from better-than-expected and worse-than-expected outcomes, forgetting of unchosen image values, learning the values of actions (e.g. if leftward choices were recently rewarded, then increase probability of leftward choices), mixtures of reinforcement learning and win-stay/lose-shift strategies, and nuisance parameters, like side bias and choice autocorrelation. We fit individual sessions using maximum likelihood estimation and selected the best model using Bayesian information criteria, which selects the best-fit model while penalizing overly complex models. The best model was among the simplest — learning of image values with equivalent learning from better/worse outcomes and a side bias mechanism (Table S1). Importantly, this model was strongly preferred over noise models (which include nuisance parameters but no learning of image values), suggesting that learning image values was consistent with real behavior. Armed with a simple and tractable model, we sought to determine how well it described real behavior.

292 First, we observed that the model fit behavioral data well (data not shown). However, model fits run the risk of
293 overfitting to data (Palminteri et al., 2017). A stronger approach is to take advantage of the generative modeling
294 framework: simulate fictive data, and assess how well simulated data matches real behavioral data. Visually,
295 we observed a correspondence between raw behavior and simulations (Figure S1B). Across all simulated monkeys,
296 we observed that simulated behavior performed better than chance, similar to real behavior (Figure 4A;
297 Wilcoxon signed-rank test, p < 0.01). Simulated behavior exhibited a dependence on reward history many trials into the past (Figure 4B). Like real monkeys, simulated monkeys were faster to transition to new Discrimination blocks than to new Reversal blocks (Figure 4C). There was no significant effect of Block Type prior to block transitions ($F_{1,96} = 0.50$, p = 0.48), which became significant after the transition ($F_{1,240} = 274.78$, p < 0.0001). Performance for Discrimination and Reversal blocks were comparable to real behavior (Figure 4D; Mean [95%CI], Discrimination: 0.685 [0.679 – 0.691], Reversal: 0.576 [0.568 – 0.584]).

303 Simulated behavior exhibited features of reward-sensitivity to images, with image-based win-stay and lose-shift both > 0.5 (Figure 4E; Wilcoxon signed-rank test, p < 0.01 for each). The average win-stay + lose-shift was > 0.5, indicating reward-sensitive behavior (Wilcoxon signed-rank test, p < 0.01) and mutual information between reward and stay/switch was similarly skewed away from 0 bits, indicating reward sensitivity (Wilcoxon signed-rank test, p < 0.01; Figure 4F,G). Simulated behavior also exhibited suboptimal features of side bias (Figure 4H; win-stay > 0.5 and lose-switch < 0.5, p < 0.01 for each). Side bias and the entropy of the side chosen distributions were similarly wide (Figure 4I,J). On a monkey-by-monkey basis, there was a strong correspondence between each of these metrics for real and simulated data (Figure S2).

311 We addressed the relationship between simulated behavioral metrics and performance. We observed a strong linear dependence between performance and average win-stay + lose-shift (Figure 5A; linear slope 0.91, $t_7 = 47.85$, p < 0.0001). There was likewise a strong association between performance and mutual information between re-

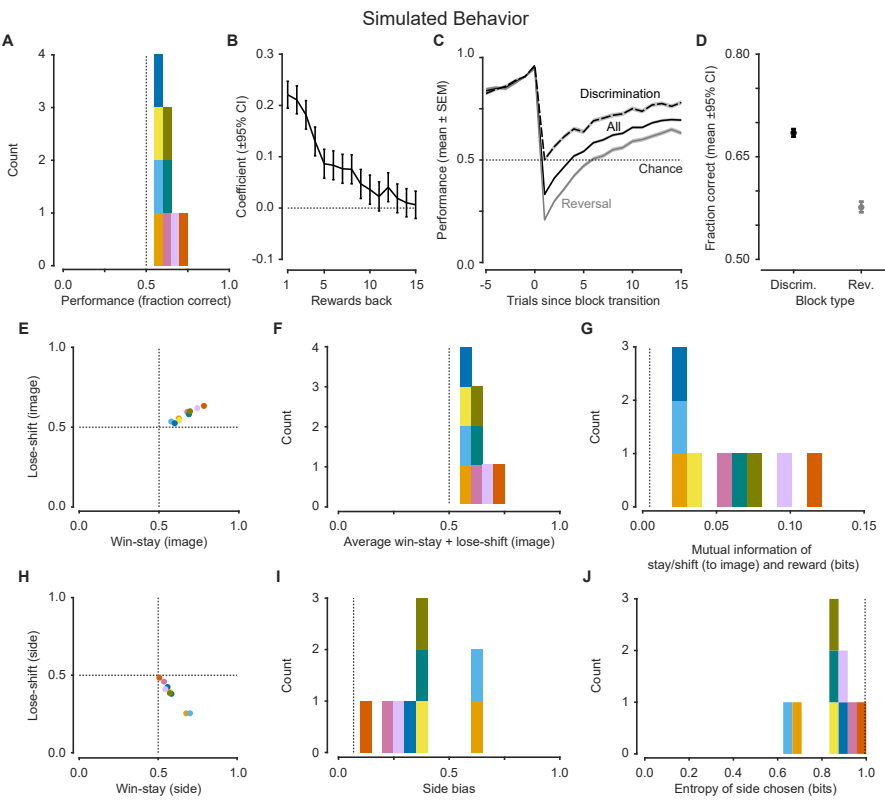


Figure 4: Simulated behavioral features demonstrate monkey-like reward sensitivity and side bias

(A) Distribution of performance was better than chance. (B) Logistic regression coefficients for choice as a function of reward history shows dependence for many trials in the past. (C) Performance at block transitions for all blocks, and separately for Discrimination and Reversal blocks. Like actual performance, pre-transition simulated data had no significant effect of Block Type which became significant after the transition. (D) Simulated performance was better in Discrimination blocks relative to Reversal blocks. (E) Image-based win-stay and lose-shift were both greater than 0.5. (F) The average win-stay + lose-shift was greater than 0.5. (G) The mutual information between stay/switch and reward on the previous trial is greater than random behavior. (H) Side-based win-stay and lose-shift demonstrates a side bias. (I) Side bias distribution. (J) The entropy of the side chosen distribution. Colors denote individual monkeys and are consistent between figures.

ward and stay/switch (Figure 5B; linear slope 0.57, $t_7 = 23.63$, $p < 0.0001$). Side bias decreased with performance (Figure 5C; linear slope -1.99 , $t_7 = -3.06$, $p = 0.18$). Entropy of the side chosen distribution similarly increased with performance (Figure 5D; linear slope 1.33, $t_7 = 2.68$, $p = 0.03$).

We also addressed the relationship between behavioral metrics and training. Simulated behavior exhibited an increase in performance with training (Figure 5E; linear slope 1.12×10^{-3} , $t_{1091} = 8.00$, $p < 0.0001$). The average win-stay + lose-shift improved with training (Figure 5F; linear slope 1.05×10^{-3} , $t_{1091} = 8.56$, $p < 0.0001$) and the mutual information between reward and stay/switch improved with training (Figure 5G; linear slope 5.44×10^{-4} , $t_{1091} = 4.65$, $p < 0.0001$). Side bias decreased with training (Figure 5H; linear slope -1.25×10^{-3} , $t_{1091} = -6.35$, $p < 0.0001$) and the entropy of the side chosen distribution similarly increased (Figure 5I; linear slope 8.10×-4 , $t_{1091} = 6.90$, $p < 0.0001$).

Taken together, these results argue that our reinforcement learning model with two core features — learning of image values, and a side bias — is sufficient to capture key features of real behavior.

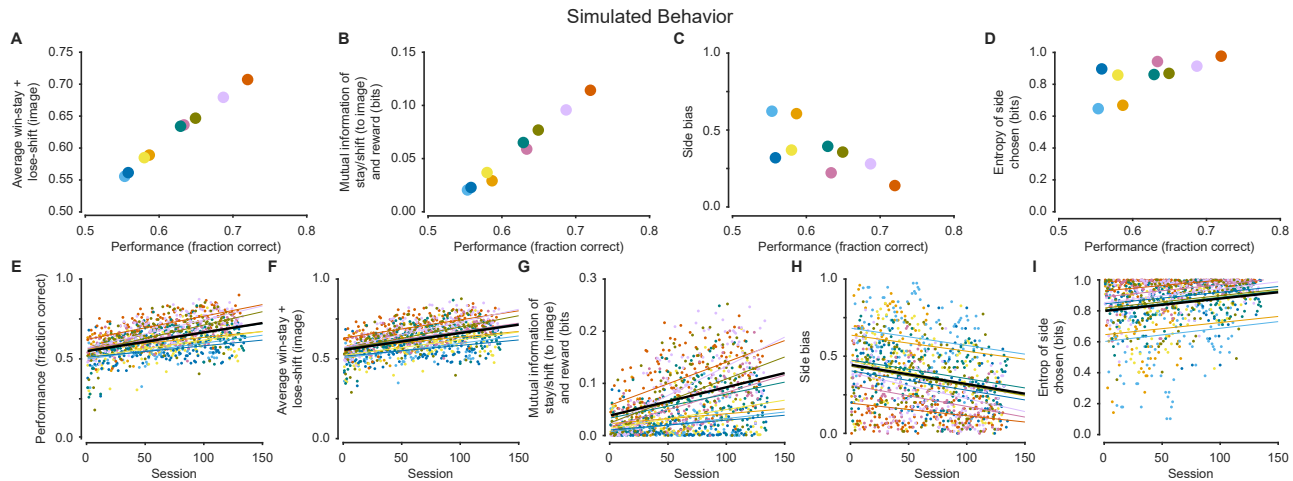


Figure 5: Simulations show similar relationships between performance, reward sensitivity, side bias, and training (A) Average win-stay + lose-shift showed a positive relationship with performance. (B) Mutual information between stay/shift and reward as a function of performance. (C) Side bias as a function of performance. (D) Entropy of side chosen as a function of performance. (E) Performance improved with training. (F) Average win-stay + lose-shift improved with training. (G) Mutual information between stay/switch and reward increased with training. (H) Side bias decreased with training. (I) Entropy of the side chosen distribution increased with training. Black line shows the fixed effect and thin colored lines show individual monkey random effects. Colors depict individual monkeys and are consistent across figures

326 Model parameters provide interpretable insight into behavioral strategy

327 A key advantage of our generative modeling approach, beyond traditional summary statistics (e.g. mean per-
328 formance, block lengths, etc), is the ability to provide intuitive explanations for how behavior was generated.
329 Our model has two key components - a learning component and a decision component. The learning component
330 determines the image values and the decision component turns the relative image values into a decision. The
331 model has three parameters, which we detail below: learning rate (α), inverse temperature (β), and side bias
332 (Figure S3A).

333 The learning rate, which affects the learning component, determines how quickly image values are updated fol-
334 lowing an outcome (Figure S3B). At its extremes, a learning rate closer to 1 means learning from only the most
335 recent trials and a learning rate closer to 0 means learning from many previous trials. In this task, higher learn-
336 ing rates are adaptive, and correspond with faster block transitions and better performance. The inverse tem-
337 perature determines choice stochasticity, or how deterministically the model acts (Figure S3C). High values of
338 inverse temperature correspond to more deterministic choice functions — the agent will opt to choose the image
339 with a higher value, even if the difference is small. Small values of inverse temperature correspond to more ran-
340 dom behavior — the agent will still choose the image with lower value with reasonable probability. In this task,
341 there is a more complex correspondence between inverse temperature and performance. High values of inverse
342 temperature correspond to behavior that better maximizes reward when the better option is known, but tends
343 to perseverate at block transitions. In general, higher values of inverse temperature correspond with better per-
344 formance. The side bias determines the model's preference for a stimulus location, regardless of relative image
345 values (Figure S3D). Nonzero values of side bias are strictly maladaptive in this task and correspond to poorer
346 performance.

347 To better estimate model parameters, we adopted a hierarchical Bayesian strategy to fit the reinforcement learn-
348 ing model and obtain monkey- and session-level parameter estimates (Figure 6A-C, S4). We related these pa-
349 rameter estimates to performance to gain better insight. We found that the learning rate improved with in-
350 creased performance (Figure 6D; linear slope 2.47, $t_7 = 7.70$, $p < 0.0001$). In contrast, the inverse temper-

ature showed no significant linear association with performance (Figure 6E; linear slope -3.23 , $t_7 = -2.00$, $p = 0.086$). Because changes in learning rates and inverse temperatures can partially compensate for one another (small increase in learning rate can be compensated for by a small decrease in inverse temperature; (Daw et al., 2011)), we sought to measure their combined effect on $P(\text{choice})$. The maximal trial-by-trial change in $P(\text{choice})$, which partially accounts for this interaction, showed an increase with performance (Figure 6F; linear slope 1.00 , $t_7 = 5.99$, $p = 5.5 \times 10^{-4}$). Finally, the absolute value of side bias showed no change with performance (Figure 6G; linear slope -5.91 , $t_7 = -1.80$, $p = 0.11$; see Discussion).

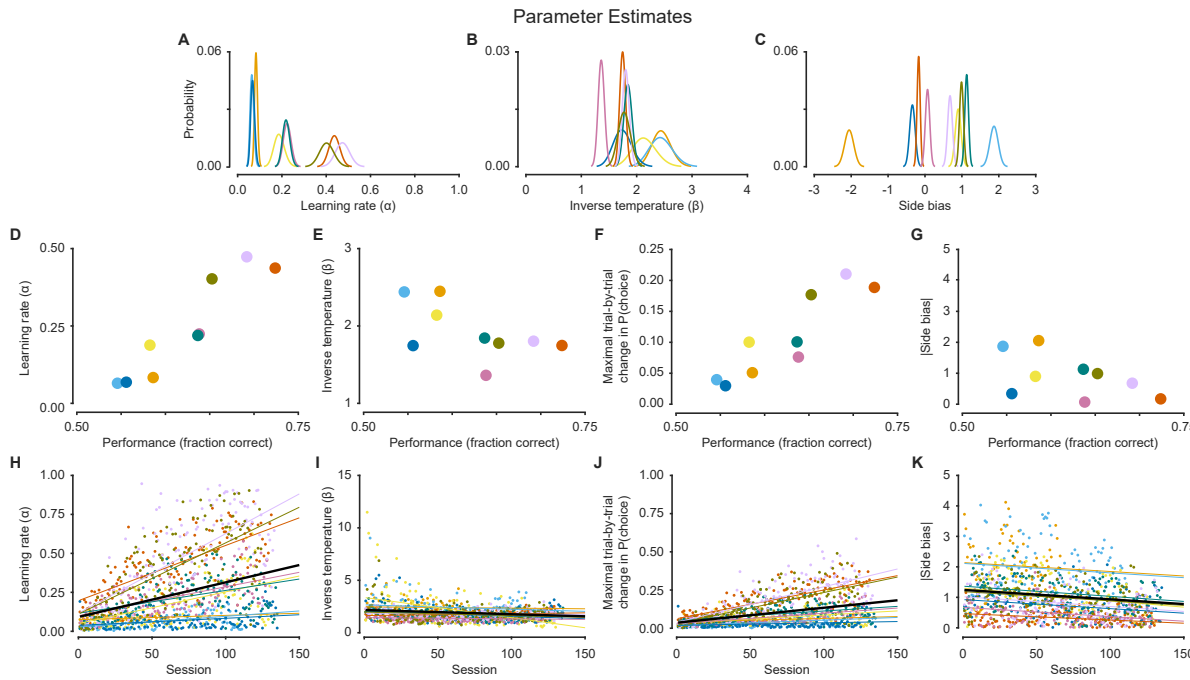


Figure 6: Relationship between model parameters, performance, and training (A) Estimate learning rates for all monkeys. (B) Estimated inverse temperatures for all monkeys. (C) Estimated side biases for all monkeys. (D) As performance improved, the learning rate increased. (E) Inverse temperature showed no significant linear association with performance. (F) The maximal trial-by-trial change in $P(\text{choice})$, which partially accounts for the interaction of both the learning rate and the inverse temperature, increased as performance improved. (G) The absolute side bias showed no significant relationship with performance. (H) Learning rates improved with training. (I) The inverse temperature did not change throughout training. (J) The maximal trial-by-trial change in $P(\text{choice})$ increased with training. (K) Side bias decreased with training. Black line shows the fixed effect and thin colored lines show individual monkey random effects. Colors denote individual monkeys and are consistent between figures.

We next sought to estimate how these parameters changed with training. Learning rates increased with training, which yields better performance (Figure 6H; linear slope 2.22×10^{-3} , $t_{1091} = 3.78$, $p = 1.7 \times 10^{-4}$). In contrast, inverse temperature showed no significant change with training (Figure 6I; linear slope -4.02×10^{-3} , $t_{1091} = -1.86$, $p = 0.06$). This is noteworthy since animals consistently adopted suboptimal inverse temperatures and would have benefited from increased β values (Figure S4; see Discussion). The maximal trial-by-trial change in $P(\text{choice})$ improved with training (Figure 6J; linear slope 9.79×10^{-4} , $t_{1091} = 3.53$, $p = 4.7 \times 10^{-4}$). Finally, side bias decreased with training, which permitted better performance (Figure 6K; linear slope -3.10×10^{-3} , $t_{1091} = -5.62$, $p < 0.0001$). We obtained similar results after within-animal normalization by z -scoring, though with a small decrease in inverse temperature with training (Figure S6).

In summary, the reinforcement modeling approach provides a simple and compelling model for understanding how squirrel monkeys solve a reversal learning task and provides a tool for interpreting how the inner mechanisms relate to performance and how they change with training.

370 Discussion

371 The power of comparative neuroscience to dissect cognition relies on the use of behavioral tasks that engage
372 similar cognitive mechanisms in different species. Here, we show that squirrel monkeys solve a reversal learning
373 task, a frequently-used behavioral paradigm, similarly to other species. We found that these animals integrate
374 reward history over many trials to dictate choices, a commonly-observed reinforcement learning motif across
375 species.

376 Using generative modeling, we explicitly tested a number of hypotheses about the strategies animals applied to
377 harvest reward. We found that animal behavior was consistent with a remarkably simple strategy: reward his-
378 tory integration over many trials (~ 5-10) and a bias for a particular side. This model outperformed a number
379 of other reasonable hypotheses. In particular, we found that a one learning rate model outperformed models
380 with two learning rates. This is notable since models with two learning rates, which allow for separate learn-
381 ing from positive and negative reward prediction errors, are commonly found to better explain behavioral data
382 (Frank et al., 2004; Grossman et al., 2020; Taswell et al., 2018; Averbeck, 2017; Dorfman et al., 2019; Gershman,
383 2015; Niv et al., 2012), although these tasks often have different reward statistics than what we used here.

384 We found that animals did not implement a pure or noisy win-stay/lose-shift strategy, either in isolation or
385 mixed with a reinforcement learning strategy. Why didn't animals approximate the optimal strategy in this
386 task? Although win-stay/lose-shift is optimal on this particular task variant, it may not be adaptive across task
387 variants in general. Reward probabilities vary drastically and dynamically in natural environments and, pre-
388 sumably, by integrating reward history, animals would continue to perform well if reward probabilities changed.
389 Reward could be optimized by tweaking parameters (e.g. adjusting learning rates), rather than changing the
390 entire behavioral strategy (Doya, 2002). Another potential reason is that incorrect choices still yielded reward,
391 allowing animals to perform well enough despite using a suboptimal strategy.

392 Monkeys did not adopt optimal combinations of learning rates and inverse temperatures to maximize reward
393 (Figure S5). Although animals had some exposure to the basics of the task (data not included), early in train-
394 ing, we would not expect animals to implement optimal parameter combinations. With training, they may ap-
395 proximate ideal parameter combinations with greater knowledge of task statistics. Indeed, we found that learn-
396 ing rates increased with training, which allows for better performance. Inverse temperatures, however, did not
397 increase, which would be expected to optimize reward. Lower inverse temperatures meant monkeys made choices
398 more randomly. This finding is consistent with the notion that monkeys maintained a high level of exploratory
399 behavior, which may be a ubiquitous feature of behavior even when task demands encourage more deterministic
400 choice behavior (Pisupati et al., 2021; Ebitz et al., 2019). Limited attention may also contribute to suboptimal
401 exploratory behavior.

402 Side-specific biases were a key feature of behavior in this task. These low-level idiosyncratic tendencies are of-
403 ten ubiquitous features of animal behavior. These side biases are likely not controlled by the same brain regions
404 that engender flexible behavior (Balleine and O'doherty, 2010; Bari et al., 2019). The reduction in side bias and
405 increase in learning rate were correlated during training (Figure 6H-K), likely because both processes yield an
406 improvement in performance, but would likely be independent following neural manipulation (Bari et al., 2019).

407 One potentially inconsistent finding is that the side bias metric decreased with performance (Figure 3C, 5C),
408 while the bias parameter from the reinforcement learning model did not show a statistically-significant change
409 (Figure 6G). This is likely because this particular analysis was underpowered. When we analyzed data at the
410 session level, we observed a significant decrease in both the mean and variance of the bias parameter (data not
411 shown). For poor performance, side bias was highly variable. This is because poor performance could be the
412 result of a strong bias to one side, or it could be the result of random, reward-insensitive behavior with no side
413 bias. With better performance, side bias decreased in mean and variance, because a strong bias places an upper
414 bound on performance, no matter how reward-sensitive animals are.

415 Generative modeling allows us to test hypotheses that may be beyond the reach of simple summary statistics.
416 For example, it is reasonable that animals could have computed action values in addition to a side bias (e.g.
417 in a task variant where computing action values may be adaptive). It's not clear how the choice-based win-
418 stay/lose-shift analyses we used (Figure 2H), which can test whether animals implement reward sensitivity to
419 choices vs side bias, would help if animals implemented a mixture of the two. With the generative modeling ap-
420 proach, as long as the model is recoverable, then this hypothesis would be simple to test (Wilson and Collins,
421 2019).

422 Our modeling approach, while generally successful, did not perfectly recapitulate all behavioral features. One
423 notable failure was the inability to capture the slight recovery of performance in the one trial immediately after
424 a Reversal block began (compare Figures 2C, 4C). Interestingly, we found that simulated data with a mixture
425 of reinforcement learning and win-stay/lose-shift was able to partially recapitulate this phenotype. However, the
426 fact that none of these models fit animal behavior well (Table S1) argues that win-stay/lose-shift is not a car-
427 dinal feature of behavior, at least given our model selection pipeline. Interestingly, win-stay/lose-shift may only
428 be a strategy animals implement on particular trials (Iigaya et al., 2017), which may disfavor a model that as-
429 sumes win-stay/lose-shift is implemented on every trial. Perhaps squirrel monkeys implement win-stay/lose-shift
430 only following large magnitude negative reward prediction errors, accounting for behavior in the trials immedi-
431 ately after a block change, and otherwise implement reinforcement learning. Learning rates might also change as
432 a function of recent reward statistics, yielding non-stationary behavioral strategies (Behrens et al., 2007; Nassar
433 et al., 2012; Grossman et al., 2020).

434 One strength of generative modeling is that it allows for interpretable insights into manipulations, particularly
435 across species. Parameter estimates (Figure S4) may be compared across groups to gain insight into the effects
436 of disease or manipulations (Kanen et al., 2021; Aylward et al., 2019; Huys et al., 2013). A complementary ap-
437 proach is to extract the latent variables governed by these parameters and correlate them with neural activity
438 (Samejima et al., 2005; Bari et al., 2019; Findling et al., 2019). Insights at the level of parameters or latent
439 variables may aid the development of novel therapies, since the development pipeline for nervous system ther-
440 apeutics often stalls due to lack of objective biomarkers of success (Kola, 2008; Paulus et al., 2016). Since these
441 types of models have theoretical underpinnings, parameter changes may be interpreted through the lens of the-
442 ory. For example, the volatility of the environment should modulate learning rates (Behrens et al., 2007), beliefs
443 about the causal structure of the environment should modulate asymmetric learning from good and bad out-
444 comes (Dorfman et al., 2019), and the complexity of action space should govern the inverse temperature and
445 perseverance (Gershman, 2020).

446 The reinforcement learning model we chose is a fairly general algorithm that is not specific to the task the mon-
447 keys performed. In fact, to best study the cognitive mechanisms underlying this algorithm across species, we
448 may need to adjust the task across species to account for species-specific differences. Humans performing a de-
449 terministic reversal learning task would almost certainly discover that win-stay/lose-shift was the optimal policy
450 and exploit it. Rhesus macaques overtrained on a deterministic reversal learning paradigm eventually learn ex-
451 pected block lengths (Jang et al., 2015). Therefore, to best study this algorithm in humans and macaques may
452 require a probabilistic reversal learning task without overtraining (to avoid win-stay/lose-shift policies), or a
453 task where the probabilities drift slowly across time, without clear reversals (to avoid learning expected block
454 lengths; (Daw et al., 2006)).

455 The behavior of squirrel monkeys is notable for the larger number of within-session reversals compared to ro-
456 dents and marmosets, which is more comparable to macaques and humans (Izquierdo et al., 2017). This means
457 that well-trained squirrel monkeys may more readily approximate human strategies, which would significantly
458 aid the ability to translate insights. Our results highlight the utility of reinforcement learning modeling and vali-
459 dates squirrel monkeys as a useful behavioral neuroscience model.

460 **Acknowledgements**

461 We thank Samantha O. Brown, and Rodrigo A. Montoro for assistance with monkey training. We thank Fred-
462 erick Barrett, Matthew Johnson, Sandeep Nayak, Manoj Doss, Justin Strickland, Ceyda Sayalı, and Cooper
463 Grossman for valuable discussions at various stages of the project. We thank Cooper Grossman for providing
464 feedback on an earlier version of the manuscript.

465 References

- 466 Abee CR. Squirrel monkey (*Saimiri* spp.) research and resources. *ILAR journal* 41: 2–9, 2000.
- 467 Averbeck BB. Amygdala and ventral striatum population codes implement multiple learning rates for reinforcement learning. In *2017 IEEE Symposium Series on Computational Intelligence (Ssci)*, pp. 1–5. IEEE, 2017.
- 468
- 469 Aylward J, Valton V, Ahn WY, Bond RL, Dayan P, Roiser JP, Robinson OJ. Altered learning under uncertainty in unmedicated mood and anxiety disorders. *Nature human behaviour* 3: 1116–1123, 2019.
- 470
- 471 Ballard IC, McClure SM. Joint modeling of reaction times and choice improves parameter identifiability in reinforcement learning models. *Journal of Neuroscience Methods* 317: 37–44, 2019.
- 472
- 473 Balleine BW, O'doherty JP. Human and rodent homologies in action control: corticostriatal determinants of goal-directed and habitual action. *Neuropsychopharmacology* 35: 48–69, 2010.
- 474
- 475 Bari BA, Grossman CD, Lubin EE, Rajagopalan AE, Cressy JI, Cohen JY. Stable representations of decision variables for flexible behavior. *Neuron* 103: 922–933, 2019.
- 476
- 477 Behrens TE, Woolrich MW, Walton ME, Rushworth MF. Learning the value of information in an uncertain world. *Nature neuroscience* 10: 1214–1221, 2007.
- 478
- 479 Boinski S. The social organizations of squirrel monkeys: Implications for ecological models of social evolution. *Evolutionary Anthropology: Issues, News, and Reviews: Issues, News, and Reviews* 8: 101–112, 1999.
- 480
- 481 Brigman JL, Ihne J, Saksida LM, Bussey T, Holmes A. Effects of subchronic phencyclidine (PCP) treatment on social behaviors, and operant discrimination and reversal learning in C57BL/6J mice. *Frontiers in behavioral neuroscience* 3: 2, 2009.
- 482
- 483
- 484 Costa VD, Dal Monte O, Lucas DR, Murray EA, Averbeck BB. Amygdala and ventral striatum make distinct contributions to reinforcement learning. *Neuron* 92: 505–517, 2016.
- 485
- 486 Crawley JN. Behavioral phenotyping strategies for mutant mice. *Neuron* 57: 809–818, 2008.
- 487
- 488 Daw ND, O'doherty JP, Dayan P, Seymour B, Dolan RJ. Cortical substrates for exploratory decisions in humans. *Nature* 441: 876–879, 2006.
- 489
- 490 Daw ND, et al. Trial-by-trial data analysis using computational models. *Decision making, affect, and learning: Attention and performance XXIII* 23, 2011.
- 491
- 492 Dawson GR, Tricklebank MD. Use of the elevated plus maze in the search for novel anxiolytic agents. *Trends in pharmacological sciences* 16: 33–36, 1995.
- 493
- 494 Den Ouden HE, Daw ND, Fernandez G, Elshout JA, Rijpkema M, Hoogman M, Franke B, Cools R. Dissociable effects of dopamine and serotonin on reversal learning. *Neuron* 80: 1090–1100, 2013.
- 495
- 496 Dorfman HM, Bhui R, Hughes BL, Gershman SJ. Causal inference about good and bad outcomes. *Psychological science* 30: 516–525, 2019.
- 497
- Doya K. Metalearning and neuromodulation. *Neural networks* 15: 495–506, 2002.
- 498
- 499 Ebitz RB, Sleezer BJ, Jedema HP, Bradberry CW, Hayden BY. Tonic exploration governs both flexibility and lapses. *PLoS computational biology* 15: e1007475, 2019.
- 500
- 501 Ersche KD, Roiser JP, Abbott S, Craig KJ, Müller U, Suckling J, Ooi C, Shabbir SS, Clark L, Sahakian BJ, et al. Response perseveration in stimulant dependence is associated with striatal dysfunction and can be ameliorated by a D2/3 receptor agonist. *Biological psychiatry* 70: 754–762, 2011.
- 502

- 503 Fenton WS, Stover EL, Insel TR. Breaking the log-jam in treatment development for cognition in schizophrenia:
504 NIMH perspective, 2003.
- 505 Findling C, Skvortsova V, Dromnelle R, Palminteri S, Wyart V. Computational noise in reward-guided learning
506 drives behavioral variability in volatile environments. *Nature neuroscience* 22: 2066–2077, 2019.
- 507 Flint J, Shifman S. Animal models of psychiatric disease. *Current opinion in genetics & development* 18: 235–
508 240, 2008.
- 509 Frank MJ, Samanta J, Moustafa AA, Sherman SJ. Hold your horses: impulsivity, deep brain stimulation, and
510 medication in parkinsonism. *science* 318: 1309–1312, 2007.
- 511 Frank MJ, Seeberger LC, O’reilly RC. By carrot or by stick: cognitive reinforcement learning in parkinsonism.
512 *Science* 306: 1940–1943, 2004.
- 513 Friedman A, Homma D, Bloem B, Gibb LG, Amemori Ki, Hu D, Delcasso S, Truong TF, Yang J, Hood AS,
514 et al. Chronic stress alters striosome-circuit dynamics, leading to aberrant decision-making. *Cell* 171: 1191–
515 1205, 2017.
- 516 Gershman SJ. Do learning rates adapt to the distribution of rewards? *Psychonomic Bulletin & Review* 22:
517 1320–1327, 2015.
- 518 Gershman SJ. Empirical priors for reinforcement learning models. *Journal of Mathematical Psychology* 71: 1–6,
519 2016.
- 520 Gershman SJ. Origin of perseveration in the trade-off between reward and complexity. *Cognition* 204: 104394,
521 2020.
- 522 Gershman SJ, Lai L. The reward-complexity trade-off in schizophrenia. *bioRxiv* , 2020.
- 523 Grossman CD, Bari BA, Cohen JY. Serotonin neurons modulate learning rate through uncertainty. *bioRxiv* ,
524 2020.
- 525 Harris C, Aguirre CG, Kolli S, Das K, Izquierdo A, Soltani A. Unique features of stimulus-based probabilistic
526 reversal learning. *bioRxiv* , 2020.
- 527 Heathcote A, Brown SD, Wagenmakers EJ. An introduction to good practices in cognitive modeling. In *An
528 introduction to model-based cognitive neuroscience*, pp. 25–48. Springer, 2015.
- 529 Huys QJ, Maia TV, Frank MJ. Computational psychiatry as a bridge from neuroscience to clinical applications.
530 *Nature neuroscience* 19: 404, 2016.
- 531 Huys QJ, Pizzagalli DA, Bogdan R, Dayan P. Mapping anhedonia onto reinforcement learning: a behavioural
532 meta-analysis. *Biology of mood & anxiety disorders* 3: 1–16, 2013.
- 533 Iigaya K, Fonseca MS, Murakami M, Mainen ZF, Dayan P. The Long and the Short of Serotonergic Stimulation:
534 Optogenetic activation of dorsal raphe serotonergic neurons changes the learning rate for rewards. *bioRxiv* p.
535 215400, 2017.
- 536 Izquierdo A, Brigman JL, Radke AK, Rudebeck PH, Holmes A. The neural basis of reversal learning: an up-
537 dated perspective. *Neuroscience* 345: 12–26, 2017.
- 538 Izquierdo A, Jentsch JD. Reversal learning as a measure of impulsive and compulsive behavior in addictions.
539 *Psychopharmacology* 219: 607–620, 2012.
- 540 Jang AI, Costa VD, Rudebeck PH, Chudasama Y, Murray EA, Averbeck BB. The role of frontal cortical and
541 medial-temporal lobe brain areas in learning a Bayesian prior belief on reversals. *Journal of Neuroscience* 35:
542 11751–11760, 2015.

- 543 Kaiser T, Feng G. Modeling psychiatric disorders for developing effective treatments. *Nature medicine* 21: 979–
544 988, 2015.
- 545 Kanen JW, Ersche KD, Fineberg NA, Robbins TW, Cardinal RN. Computational modelling reveals contrasting
546 effects on reinforcement learning and cognitive flexibility in stimulant use disorder and obsessive-compulsive
547 disorder: remediating effects of dopaminergic D2/3 receptor agents. *Psychopharmacology* 236: 2337–2358,
548 2019.
- 549 Kanen JW, Luo Q, Kandroodi MR, Cardinal RN, Robbins TW, Carhart-Harris RL, den Ouden HE. Effect of
550 lysergic acid diethylamide (LSD) on reinforcement learning in humans. *bioRxiv* pp. 2020–12, 2021.
- 551 Kola I. The state of innovation in drug development. *Clinical Pharmacology & Therapeutics* 83: 227–230, 2008.
- 552 Leeson VC, Robbins TW, Matheson E, Hutton SB, Ron MA, Barnes TR, Joyce EM. Discrimination learning,
553 reversal, and set-shifting in first-episode schizophrenia: stability over six years and specific associations with
554 medication type and disorganization syndrome. *Biological psychiatry* 66: 586–593, 2009.
- 555 Markou A, Chiamulera C, Geyer MA, Tricklebank M, Steckler T. Removing obstacles in neuroscience drug dis-
556 covery: the future path for animal models. *Neuropsychopharmacology* 34: 74–89, 2009.
- 557 Mason L, Eldar E, Rutledge RB. Mood instability and reward dysregulation—a neurocomputational model of
558 bipolar disorder. *JAMA psychiatry* 74: 1275–1276, 2017.
- 559 Metha JA, Brian ML, Oberrauch S, Barnes SA, Featherby TJ, Bossaerts P, Murawski C, Hoyer D, Jacobson
560 LH. Separating probability and reversal learning in a novel Probabilistic Reversal Learning task for mice.
561 *Frontiers in behavioral neuroscience* 13: 270, 2020.
- 562 Michely J, Eldar E, Martin IM, Dolan RJ. A mechanistic account of serotonin's impact on mood. *Nature com-*
563 *munications* 11: 1–11, 2020.
- 564 Nassar MR, Rumsey KM, Wilson RC, Parikh K, Heasly B, Gold JI. Rational regulation of learning dynamics by
565 pupil-linked arousal systems. *Nature neuroscience* 15: 1040, 2012.
- 566 Nestler EJ, Gould E, Manji H. Preclinical models: status of basic research in depression. *Biological psychiatry*
567 52: 503–528, 2002.
- 568 Niv Y, Edlund JA, Dayan P, O'Doherty JP. Neural prediction errors reveal a risk-sensitive reinforcement-
569 learning process in the human brain. *Journal of Neuroscience* 32: 551–562, 2012.
- 570 O'Doherty J, Dayan P, Schultz J, Deichmann R, Friston K, Dolan RJ. Dissociable roles of ventral and dorsal
571 striatum in instrumental conditioning. *science* 304: 452–454, 2004.
- 572 Ottenheimer DJ, Bari BA, Sutlief E, Fraser KM, Kim TH, Richard JM, Cohen JY, Janak PH. A quantitative
573 reward prediction error signal in the ventral pallidum. *Nature neuroscience* 23: 1267–1276, 2020.
- 574 O'Shea DJ, Kalanithi P, Ferenczi EA, Hsueh B, Chandrasekaran C, Goo W, Diester I, Ramakrishnan C, Kauf-
575 man MT, Ryu SI, et al. Development of an optogenetic toolkit for neural circuit dissection in squirrel monkeys.
576 *Scientific reports* 8: 1–20, 2018.
- 577 Palminteri S, Wyart V, Koechlin E. The importance of falsification in computational cognitive modeling. *Trends*
578 *in cognitive sciences* 21: 425–433, 2017.
- 579 Pangalos MN, Schechter LE, Hurko O. Drug development for CNS disorders: strategies for balancing risk and
580 reducing attrition. *Nature Reviews Drug Discovery* 6: 521–532, 2007.
- 581 Paulus MP, Huys QJ, Maia TV. A roadmap for the development of applied computational psychiatry. *Biological*
582 *psychiatry: cognitive neuroscience and neuroimaging* 1: 386–392, 2016.

- 583 Pike AC, Lowther M, Robinson OJ. The Importance of Common Currency Tasks in Translational Psychiatry.
584 *Current Behavioral Neuroscience Reports* pp. 1–10, 2021.
- 585 Pisupati S, Chartarifsky-Lynn L, Khanal A, Churchland AK. Lapses in perceptual decisions reflect exploration.
586 *Elife* 10: e55490, 2021.
- 587 Porter JN, Olsen AS, Gurnsey K, Dugan BP, Jedema HP, Bradberry CW. Chronic cocaine self-administration
588 in rhesus monkeys: impact on associative learning, cognitive control, and working memory. *Journal of Neuro-*
589 *science* 31: 4926–4934, 2011.
- 590 Radulescu A, Niv Y. State representation in mental illness. *Current opinion in neurobiology* 55: 160–166, 2019.
- 591 Redish AD. Addiction as a computational process gone awry. *Science* 306: 1944–1947, 2004.
- 592 Remijnse PL, Nielen MM, van Balkom AJ, Cath DC, van Oppen P, Uylings HB, Veltman DJ. Reduced
593 orbitofrontal-striatal activity on a reversal learning task in obsessive-compulsive disorder. *Archives of general*
594 *psychiatry* 63: 1225–1236, 2006.
- 595 Rescorla RA. A theory of Pavlovian conditioning: Variations in the effectiveness of reinforcement and nonrein-
596 forcement. *Current research and theory* pp. 64–99, 1972.
- 597 Samejima K, Ueda Y, Doya K, Kimura M. Representation of action-specific reward values in the striatum. *Sci-
598 ence* 310: 1337–1340, 2005.
- 599 Schultz W, Dayan P, Montague PR. A neural substrate of prediction and reward. *Science* 275: 1593–1599, 1997.
- 600 Soltani A, Izquierdo A. Adaptive learning under expected and unexpected uncertainty. *Nature Reviews Neuro-
601 science* 20: 635–644, 2019.
- 602 Sutton RS, Barto AG. *Reinforcement Learning: An Introduction*. MIT Press Cambridge, 1998.
- 603 Swainson R, Rogers R, Sahakian B, Summers B, Polkey C, Robbins T. Probabilistic learning and reversal
604 deficits in patients with Parkinson's disease or frontal or temporal lobe lesions: possible adverse effects of
605 dopaminergic medication. *Neuropsychologia* 38: 596–612, 2000.
- 606 Tallman JF. Neuropsychopharmacology at the new millennium: new industry directions. *Neuropsychopharma-
607 cology* 20: 99–105, 1999.
- 608 Taswell CA, Costa VD, Murray EA, Averbeck BB. Ventral striatum's role in learning from gains and losses.
609 *Proceedings of the National Academy of Sciences* 115: E12398–E12406, 2018.
- 610 Wilson RC, Collins AG. Ten simple rules for the computational modeling of behavioral data. *Elife* 8: e49547,
611 2019.

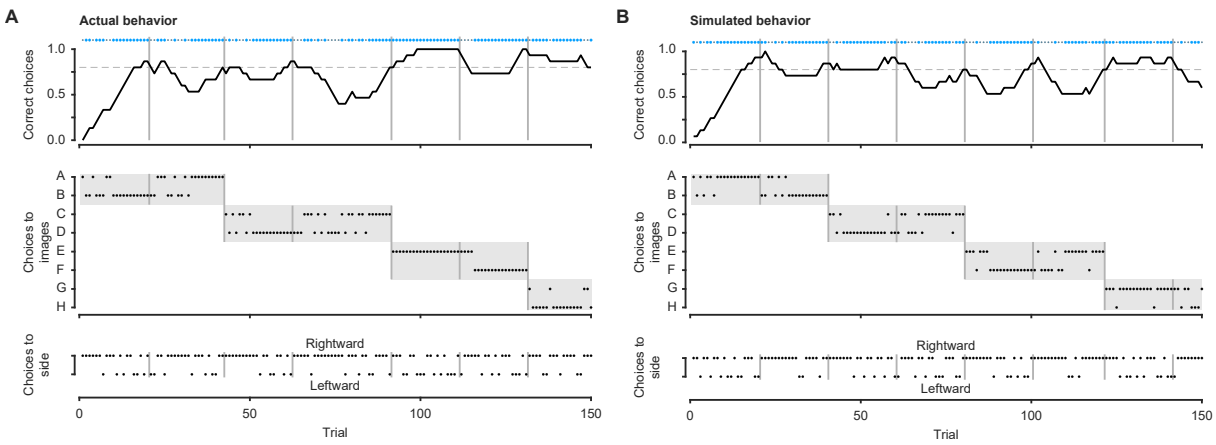


Figure S1: Raw behavior for actual and simulated sessions (A) Top panel: Correct choices as a function of trial. Large dots indicate a big reward choice and small dots indicate a small reward choice. The black line shows the fraction correct in the past 15 trials. The dashed line is the performance threshold (80% correct) used to trigger block transitions. Vertical grey lines indicate block transitions. Middle panel: Choices to images as a function of trial in the same format as 1C. Black dots indicate a choice to a respective image. Bottom: Choices to a side as a function of trial. Rightward (leftward) choices are indicated with a black dot on the top (bottom) of the figure. This session demonstrates a slight rightward side bias. (B) Behavior from the same session was fit to the reinforcement learning model to estimate parameters. These parameters were used to simulate an entirely new, synthetic data session.

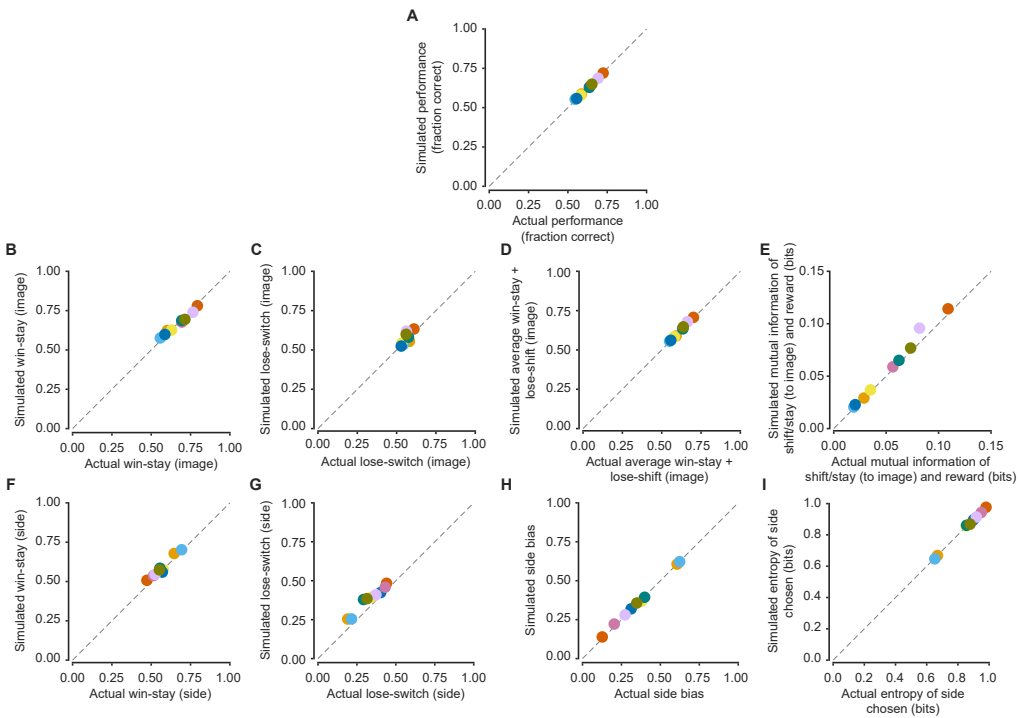


Figure S2: Comparison of behavioral features for actual and simulated behavior. To compare how well actual and simulated behavioral features match, we compute the mean difference between actual and simulated behavioral features [Mean (actual minus simulated) 95% CI] for each panel. (A) Average performance for each session. [-0.0015 – 0.0042] (B) Image-based win-stay [-0.0070 – 0.0130] (C) Image-based lose-shift [-0.0303 – 0.0015] (D) Image-based average win-stay + lose-shift [-0.0043 – 0.0064] (E) Mutual information of stay/shift and reward on the previous trial [-0.0082 – -0.0021] (F) Side-based win-stay [-0.0265 – -0.0062] (G) Side-based lose-shift [-0.0632 – -0.0367] (H) Side bias [-0.0097 – 0.0015] (I) Entropy of side chosen distribution [-0.0012 – 0.0052]. Colors denote individual monkeys and are consistent between figures.

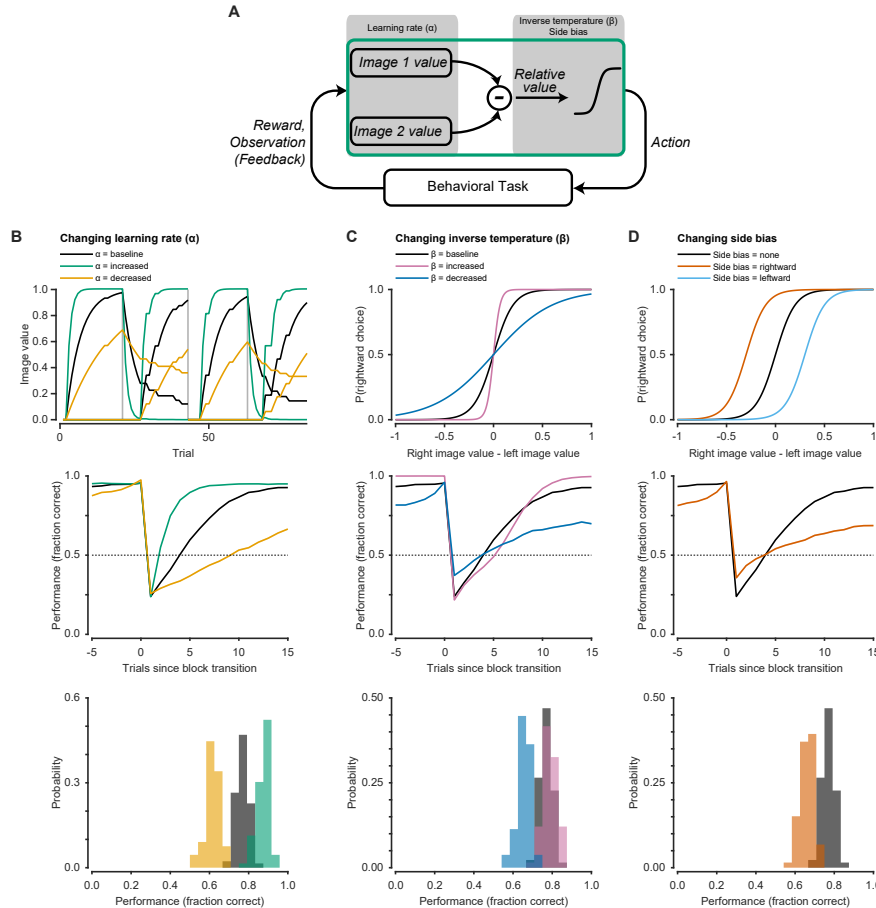


Figure S3: Model illustration and effects of varying parameters (A) Illustration of reinforcement learning model. Image values are updated by feedback via reward prediction errors (the discrepancy between predicted and actual rewards). This process is governed by the learning rate (α). The relative image value is mapped through a softmax function to produce a choice. This process is governed by the inverse temperature (β) and a side bias parameter. (B) Increasing the learning rate results in faster accumulation of reward value information. This results in faster block transitions and better overall performance. Decreasing the learning rate has the opposite effect. (C) Increasing the inverse temperature results in more deterministic choice behavior. Decreasing the inverse temperature makes choices more random. In this example, increasing the inverse temperature results in slower block transitions but more deterministic behavior after enough trials have elapsed, resulting in improved performance. Decreasing the inverse temperature has the opposite effect. Unlike the learning rate, the optimal inverse temperature is not at an extreme value but depends on the trials to criterion. Greater trials to criterion will favor a larger β . (D) Side bias results in increased choices of one particular side. Side bias is purely maladaptive and results in poorer overall performance.

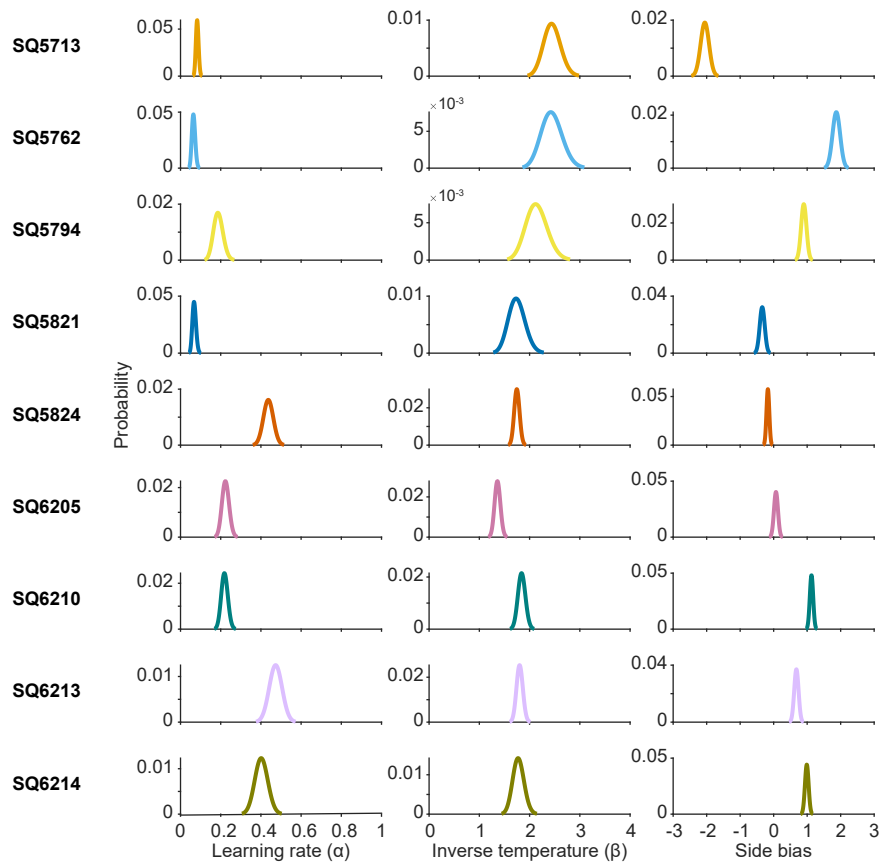


Figure S4: Parameter estimates for each monkey. Estimated learning rates, inverse temperatures, and side biases for all monkeys included in this study. Colors indicate the color used for that monkey throughout figures.

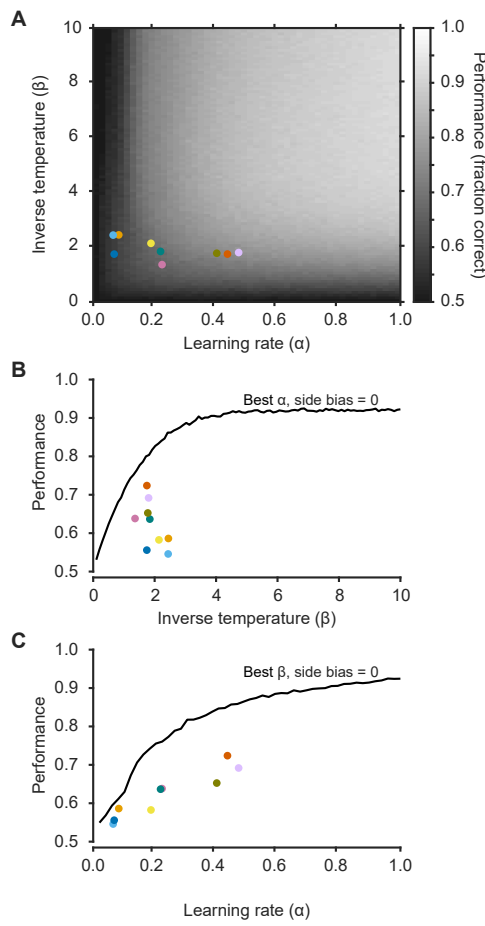


Figure S5: Performance as a function of learning rate (α) and inverse temperature (β). Each simulation was run for 66 sessions, each 2000 trials long, over 50 α values, 100 β values, and side bias fixed at 0. (A) Heatmap of performance for combinations of learning rates and inverse temperatures, with side bias fixed at 0. Performance is poor at low learning rates (regardless of the inverse temperature) and low inverse temperatures (regardless of the learning rate). In general, there is a large range of learning rates and inverse temperatures that permits adaptive behavior. Individual monkeys are shown with colored dots. Monkeys consistently maintain a suboptimal α/β combination. (B) Performance as a function of inverse temperature for the best learning rate and side bias = 0. Optimal performance is achieved at $\beta \gtrsim 4$. (C) Performance as a function of learning rate for the best inverse temperature and side bias = 0. Optimal performance is achieved at $\alpha = 1$. Colors denote individual monkeys and are consistent between figures.

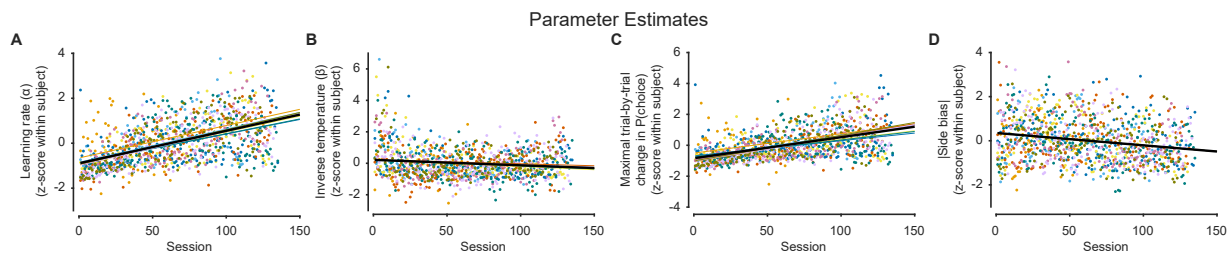


Figure S6: Within-subject normalization of parameters results in similar changes with training

(A) Normalized learning rates improved with training (linear slope 1.44×10^{-2} , $t_{1091} = 17.33$, $p < 0.0001$). (B) Normalized inverse temperatures decreased with training (linear slope -3.46×10^{-3} , $t_{1091} = -4.05$, $p < 0.0001$). (C) Normalized maximal change in P(choice) increased with training (linear slope 1.36×10^{-2} , $t_{1091} = 11.13$, $p < 0.0001$). (D) Normalized absolute side bias decreased throughout training (linear slope -5.61×10^{-3} , $t_{1091} = -7.11$, $p < 0.0001$). Colors denote individual monkeys and are consistent between figures.

Monkey	Model									
	RW + Side bias (3 parameters)		RW + Side bias + Reversal mechanism (3 parameters)		RW + Side bias + Forget unchosen (4 parameters)		RW + Side bias + Forget unchosen + reward coded as [0.25 1] (4 parameters)		Side bias (1 parameter)	
	LH	BIC	LH	BIC	LH	BIC	LH	BIC	LH	BIC
SQ5713	3685	8363	3756	8505	3639	8601	3638	8598	4586	9503
SQ5762	6271	14198	6366	14389	6152	14513	6114	14438	7288	15129
SQ5794	9139	20186	9239	20385	8833	20211	8791	20127	10595	21826
SQ5821	11387	24796	11512	25046	11310	25315	11272	25240	12446	25566
SQ5824	9588	21135	9522	21003	9260	21132	9285	21181	13089	26831
SQ6205	10776	23475	10801	23525	10583	23728	10585	23732	12573	25786
SQ6210	9483	20988	9559	21140	9199	21093	9223	21141	11835	24344
SQ6213	9341	20675	9313	20619	8750	20157	8777	20212	12556	25777
SQ6214	8535	18925	8591	19037	8091	18655	8085	18645	11073	22764

Table S1: Model comparison. Comparison of negative log likelihood (LH) and Bayesian information criterion (BIC) values for the four models best fit to at least one monkey, and one noise model. The four best-fit models are variations of the Rescorla-Wagner (RW) model with a side bias. The noise model is a side bias only model. LH and BIC values are sums across all sessions for individual monkeys. Colors in the Monkey column indicate the color used for that monkey throughout figures. Gray highlights the best model (smallest BIC) for each monkey.